HAL
open science

Lanthanide containing ionic liquid crystals: EuBr2, SmBr3, TbBr3 and DyBr3 in C12mimBr

Anja-Verena Mudring

To cite this version:

Anja-Verena Mudring. Lanthanide containing ionic liquid crystals: EuBr2, SmBr3, TbBr3 and DyBr3 in C12mimBr. Journal of Inorganic and General Chemistry / Zeitschrift für anorganische und allgemeine Chemie, 2010, 636 (9-10), pp.1726. 10.1002/zaac.201000070 . hal-00552457

HAL Id: hal-00552457

https://hal.science/hal-00552457v1

Submitted on 6 Jan 2011

HAL is a multi-disciplinary open access archive for the deposit and dissemination of scientific research documents, whether they are published or not. The documents may come from teaching and research institutions in France or abroad, or from public or private research centers.

L'archive ouverte pluridisciplinaire **HAL**, est destinée au dépôt et à la diffusion de documents scientifiques de niveau recherche, publiés ou non, émanant des établissements d'enseignement et de recherche français ou étrangers, des laboratoires publics ou privés.

Zeitschrift für Anorganische und Allgemeine Chemie

Lanthanide containing ionic liquid crystals: EuBr2, SmBr3, TbBr3 and DyBr3 in C12mimBr

Journal:	*Zeitschrift für Anorganische und Allgemeine Chemie*
Manuscript ID:	zaac.201000070.R1
Wiley - Manuscript type:	Article
Date Submitted by the Author:	14-Mar-2010
Complete List of Authors:	Mudring, Anja-Verena; Ruhr-Universitaet Bochum, Anorganische Chemie I
Keywords:	Ionic Liquids, Liquid Crystals, Luminescence, Lanthanides

scholarONE™
Manuscript Central

DOI: 10.1002/zaac.2008

Lanthanide containing ionic liquid crystals: $EuBr_2$, $SmBr_3$, $TbBr_3$ and $DyBr_3$ in C_{12}mimBr

Anna Getsis and Anja-Verena Mudring*

Bochum, Fakultät für Chemie und Biochemie, Anorganische Chemie I, Festkörperchemie und Materialien, Ruhr-Universität Bochum

Received

Dedicated to Professor Bernd Harbrecht on the Occasion of his 60th Birthday.

Abstract. Doping the ionic liquid crystal C_{12}mimBr with various lanthanide halides yields interesting novel liquid crystalline and luminescent materials. The thermal phase behavior of all compounds was investigated by hot-stage polarizing optical microscopy and differential scanning calorimetry and the photophysical properties were determined by luminescence spectroscopy. C_{12}mimBr itself is an ionic liquid crystal that shows bluish-white emission upon excitation with UV light due to transitions in the imidazolium π-system. Doping lanthanide bromides into C_{12}mimBr with concentrations of about 1 mol% does not affect the liquid crystalline behaviour of the host materials to a great extent and room temperature liquid crystals are obtained. All materials show an appreciable luminescence. $EuBr_2$ in C_{12}mimBr yields a material which shows a blue emission originating from 4*f*-5*d*-transitions. $SmBr_3$-doped samples show a red and $TbBr_3$ samples a green luminescence. Upon doping C_{12}mimBr with $DyBr_3$ an orange luminescent liquid crystalline material is obtained. Most interestingly the emission color for the $TbBr_3$ and $DyBr_3$ containing materials can be tuned from bluish-white (mainly C_{12}mimBr emission) to green (for $TbBr_3$) and orange-yellow (for $DyBr_3$) depending on the wavelength of the excitation light used.

Keywords: Dysprosium; Europium; Ionic Liquid; Liquid Crystal; Luminescence; Samarium; Terbium

Introduction

Although ionic liquids (ILs) have received an exceptionally high attention as a new class of solvents and materials for various applications, the understanding of interactions within these liquids is still rather limited. It has been noted from early on that ILs are highly structured liquids[1]. Ionic liquid crystals (ILCs) represent a special class of ILs where weak hydrophobic interactions of alkyl groups, dipole–dipole, cation–π interactions as well as π–π stacking of the commonly used aromatic head groups of the cation such as imidazolium or pyridinium as well as ionic interactions are tremendously important and are the driving force for the formation of ordered liquids, hence, liquid crystalline phases.

The liquid crystalline state of matter shows characteristics which are intermediate between that of a three-dimensionally well ordered crystalline solid and an isotropic liquid where the constituents are distributed randomly through space.[2] Generally, in the liquid crystalline state a random distribution of particles - like in a classical liquid - is observed at least in one direction of space whereas in another direction a substantially higher degree of order is observed which comes close to the periodicity of crystalline materials. Typically, many of the physicochemical properties of liquid crystals (LCs) such as refractive index, electric permittivity, magnetic susceptibility, and mechanical properties like viscosities are highly depent on the direction in which these properties are measured. This has shown to be useful for a wide variety of applications and, in consequence, molecular liquid crystalline materials have found widespread applications in display technology in laptops, mobile phones, or flat screen television sets.[3]

Whilst most known liquid crystals are neutral molecular organic compounds of strong anisotropic shape, ionic liquid crystals (ILCs) are constituted of anions and cations. Mesophasic behaviour can be introduced into such an ionic material via either one of the ions. It is known that 1-alkyl-3-methylimidazolium salts with twelve and more carbon atoms in the side chain adopt mesophases and that the mesophase stability rapidly increases with increase in the alkyl chain length[4]. Most times, a lamellar mesophase, a smectic A phase or other highly ordered smectic phases are observed. It has been realized that ILCs show unique characteristics that cannot be observed in conventional molecular LCs. In ILCs a

*Prof. Dr. Anja-Verena Mudring
Ruhr-Universität Bochum, Fakultät für Chemie und Biochemie; Anorganische Chemie I – Festkörperchemie und Materialien
D-44780 Bochum
www.anjamudring.de

tetragonal smectic phase S_T was observed for the first time.[5] Recently, it was shown that double alkyl substituted imidazolium ILCs show strong non-Newtonian fluidic behavior in the LC state while they are Newtonian liquids in the liquid IL state.[6] ILCs also show a strong tendency for spontaneous homeotropic alignment.[7] Applications of ionic liquid crystals are, so far, as ion-conductive materials, organized reaction media or self-assembled nanostructured materials.[8]

Metal-containing liquid crystals (metallomesogens) form a special class of ILCs. By choosing a suitable metal ion as the ILC constituent additional functionalities that origin from the metals such as redoxactivity, magnetism or luminescence can be introduced into the material. In consequence, multifunctional materials are obtained. Several reviews survey the intensive studies on neutral, uncharged metallomesogens.[9] In contrast studies of ionic metallomesogens have been neglected until recently[10, 11]. Metal based ionic liquid crystals are known for various transition metals. The majority of the metal-containing ionic liquids have the $[MX_4]^{2-}$ structural building block with M = Co, Ni, Cu, Zn, Pd, Cd and X=Cl, Br and sometimes I. Typical counter cations are long-chain quaternary ammonium cations,[12, 13, 14, 15] N-alkylpyrrolidinium,[16] *N*-alkylpyridinium cations,[17, 18, 19, 20, 21, 22] and 1-alkyl-3-methylimidazolium cations[23] Lanthanide based ILCs such as $[C_{12}mpyr]_3[TbBr_3]$ ($C_{12}mpyr$ = N-dodecyl-N-methylimidazolium),[24] $[C_{12}mim]_3LnBr_6$ ($C_{12}mim$ = 1-dodecyl-3-methylimidazolium; Ln = Dy, Tb)[25] or $[C_{12}mim]_4[EuBr_6]Br$.[26]

Special interest in the field of such metal-containing liquid crystals focuses on light emitting liquid crystals for potential applications in emissive LC displays.[27] By incorporating 4f-element cations such as Eu^{2+} or Tm^{3+} for blue, Eu^{3+} or Sm^{3+} for red and Tb^{3+} for green emission LCs emitting in the three basic colors can be obtained.[28] In addition, aligned luminescent LCs can emit polarized light.[29] A high magnetic anisotropy of the lanthanide ion as found for Tb^{3+}, Dy^{3+} and Tm^{3+} makes the alignment of the mesophase in an external magnetic field possible.[30] Thus, such compounds might be of interest for the use of electric and magnetic switchable devices.[31] However, aside from lanthanide-based ILCs another viable way to ionic liquid crystalline material which shows lanthanide emission is to dope ILCs with suitable lanthanide salts.

Here we report on $C_{12}mimBr$, a well known ionic liquid crystal[32], doped with $EuBr_2$, $SmBr_3$, $TbBr_3$ and $DyBr_3$, which allows to obtain ILC materials which show luminescence in the three basic colors. The luminescence properties of the obtained hybrid materials are investigated by luminescence spectroscopy. The thermal behaviour and mesophase formation is investigated by combined thermal (differential scanning calorimetry, DSC) and temperature dependent polarized optical microscopy (POM).

Experimental details.

Handling of $C_{12}mimBr$ and $EuBr_2$ as well as $LnBr_3$ (Ln Pr, Sm, Tb, Dy) containing samples was carried out under strict inert conditions (vacuum, argon) using advanced Schlenk and glove-box techniques.

1-Dodecyl-3-methylimidazolium bromide, $C_{12}mimBr$. For $C_{12}mimBr$ 0.1 mol methylimidazole (99 %, ABCR GmbH&Co, Karlsruhe, D) is dissolved in 70 ml dry acetonitrile. Then 0.1 mol n-dodecylbromide (99 % Acros organics, Geel, B) is added drop-wise and the reaction mixture is heated under reflux for 18 h. After cooling to room temperature most of the solvent is removed under vacuum. Upon adding the concentrated acetonitrile solution to 300 ml cold (-30°C) and dry toluene, 1-dodecyl-3-methylimidazolium bromide precipitates as a white powder. The reaction product is filtered off and re-crystallized two times from dry acetonitrile/toluene. The product is dried from any remaining solvent for 48 h under dynamic vacuum. Yield: ~70 %.

δ_H (298 K, 300 MHz, DMSO-d_6): 0.868 [t, 3H, H-1]; 1.234 [br. S., 18H, H-2]; 1.766 [quint., 2H, H-3]; 3.848 [s, 3H, H-5]; 4.149 [t, 2H, H-4]; 7.708 [m,1H, H-6]; 7.777 [m, 1H, H-7]; 9.151 [br. S., 1H, H-8].

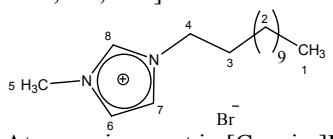

Scheme 1. Atom assignment in $[C_{12}mim]Br$ (**1**).

MIR (KBr pellet): / [cm^{-1}] = 3226.5 (w), 3149.4 (m), 3083.8 (s), 3062.6 (s), 2950.7 (s), 2916.0 (s), 2869.7 (s), 2852.4 (s),1772.4 (w), 1668.2 (w), 1629.7 (m), 1571.8 (m), 1473.4 (m), 1427.2 (w), 1384.7 (w), 1344.2 (w), 1317.2 (w), 1292.2 (w), 1178.4 (s), 1126.3 (w), 1089.7 (w), 1054.9 (w), 1043.4 (w), 1022.2 (w), 1004.8 (w), 943.1 (w), 887.2 (w, shoulder), 862.1 (m), 792.6 (m), 763.7 (w), 742.5 (w), 729.0 (w), 715.5 (m), 661.5 (m), 622.9 (m).

FIR (PE pellet): / [cm^{-1}] = 562.2 (m, shoulder), 509.1 (w), 498.9 (w), 472.5 (w), 453.2 (m), 417.5 (m), 396.3 (m), 349.1 (w), 284.5 (w), 230.5 (w), 154.3 (m, shoulder), 93.5 (s), 64.6 (s, shoulder).

Raman: / [cm^{-1}] = 3134.2 (w), 3082.9 (w), 2956.7 (w), 2933.6 (s), 2883.5 (s), 2848.7 (s), 2727.2 (w), 1560.4 (vw), 1452.4 (w, shoulder), 1432.1 (w), 1421.6 (w, shoulder). 1375.3 (vw), 1334.8 (vw), 1296.2 (w), 1128.4 (w), 1105.3 (vw), 1087.9 (vw), 1062.9 (w), 1014.6 (w), 887.4 (vw), 733.1 (vw), 692.6 (vw), 654.0 (vw), 605.8 (vw), 414.9 (vw), 303.0 (vw), 231.6 (vw), 181.5 (vw, shoulder), 150.6 (w, shoulder), 114.0 (w), 85.1 (w, shoulder).

Elemental analysis (%) calcd for $[C_{12}mim]Br$: C 58.00, H 9.43, N 8.45; found: C 57.63, H 9.74, N 8.42.

$EuBr_2$. According to a literature procedure[33] 2.8 g (8 mmol) europium(III) oxide (99.97%, Fluka Chemie, Buchs, CH) are dissolved in 80 ml conc. HBr (48%, Aldrich, Steinheim, D) and 11 g (0.112 mol) ammonium bromide (99.995%, Merck, Darmstadt, D) are added. After all starting materials are dissolved the solvent is boiled off. The residual yellow solid is heated under vacuum at 120 °C (20 °C/h) for 6 h, then at 400 °C (20 °C/h) for 12 h before cooling to room temperature (20 °C/h). The obtained $EuBr_2$ is checked for identity and purity by PXRD (powder X-ray diffraction).

$LnBr_3$ (Ln = Sm, Tb, Dy). $LnBr_3$ was synthesised according to a modified literature procedure.[34] For $SmBr_3$ and $DyBr_3$ 0.005 mol of the respective lanthanide(III) oxide (99.9% Fluka Chemie AG, Buchs, CH) and 0.07 mol ammonium bromide (suprapur® 99.995% Merck, Darmstadt, D), for $TbBr_3$ 0.004 mol Tb_4O_7 (99.9% Fluka Chemie AG, Buchs, CH) and 0.102 mol ammonium bromide were dissolved in 48% conc. aqueous hydrobromic acid (Aldrich, Steinheim, D). After removing the solvent, the formed $(NH_4)_3LnBr_6 \cdot yH_2O$ is decomposed to $LnBr_3$ at elevated temperatures where also any excess of ammonium bromide sublimes of. The crude $LnBr_3$ is then purified by sublimation under vacuum (< 10^{-5} mbar). The purity of the obtained $LnBr_3$ is checked by PXRD.

LnX_2/LnX_3 in C_{12}mimBr. To obtain lanthanide halide containing C_{12}mimBr samples the respective amounts of the lanthanide bromide and 1-dodecyl-3-methylimidazolium bromide are heated in a sealed silica ampoule under vacuum at 120°C until a homogeneous mixture is obtained. After cooling to room temperature waxy solids are obtained which are subjected to further analysis. Alternatively the lanthanide halide and C_{12}mimBr can be dissolved in CH_2Cl_2 at room temperature. After removal of the solvent under vacuum, again, waxy samples of the desired composition are obtained.

Instrumentation. Elemental analyses were obtained on an Euro Vektor elemental analyzer EuroEA 3000 (HEKAtech GmbH, Wegberg, D) for C_{12}mimBr.

^{1}H-Nuclear magnetic resonance (NMR) spectra were recorded on a Bruker AC-300 spectrometer (operating at 300 MHz for ^{1}H) (Bruker Germany GmbH, D).

IR spectra of the solid were recorded using a IFS-66V-S Fourier Transform IR spectrometer (Bruker Optik GmbH, Ettlingen, D); samples were measured pressed in a polyethylene matrix for far IR range (50-600 cm^{-1}) and in a KBr matrix for middle IR (MIR) range (600-4000 cm^{-1}).

Raman spectra were recorded with a FRA 106-S Fourier Transform Raman spectrometer (Bruker Optik GmbH, Ettlingen, D) at 150mW. Raman samples were measured in glass capillaries with an inner diameter of 0.1 cm and 0.15 mm wall thickness.

Differential scanning calorimetry (DSC) was performed with a computer-controlled Phoenix DSC 204 F1 thermal analyser (Netzsch, Selb, D) with argon as protection gas. The samples were placed in aluminium pans which were cold-sealed under argon. Experimental data are displayed in such a way that exothermic peaks occur at negative heat flow and endothermic peaks at positive heat flow. Heating and cooling rates were 5°C/min. Given temperatures correspond to the onset of the respective thermal process.

Optical polarizing microscopy was carried out with an Axio Imager A1 microscope (Carl Zeiss MicroImaging GmbH, Göttingen, D) equipped with a hot stage THMS600 (Linkam Scientific Instruments Ltd, Surrey, UK) and a temperature controller Linkam TMS 94 (Linkam Scientific Instruments Ltd, Surrey, UK) and crossed polarizers. Images were recorded at a magnification of 100× as movies with a digital camera after initial heating during the cooling stage. Heating and cooling rates were 5 K/min^{-1}. For the measurement the samples were placed under argon between two cover slips which were sealed with a two-component adhesive (UHU plus 300, UHU GmbH & Co. KG, Bühl, D).

UV-Vis spectra were obtained with a Cary 5000 spectrometer (Bruker, Bremen, Germany) at room temperature. Excitation and emission spectra and also luminescence decays were recorded on a Jobin Yvon Horiba Fluorolog FL3-22 (HORIBA Jobin Yvon Inc., Unterhaching, D) with a xenon lamp as the excitation source and a photomultiplier tube for detection. Interconfigurational f-f-transitions are assigned according to the Dieke diagram.[35]

Results and Discussion

C_{12}mimBr

Dry C_{12}mimBr was chosen as a host matrix with liquid crystalline properties and doped with various amounts of $EuBr_2$, $SmBr_3$, $TbBr_3$ and $DyBr_3$.

DSC measurements show that upon cooling liquid samples of C_{12}mimBr from the isotropic melt a liquid to liquid crystalline (L↔LC) phase transition occurs at 99.2°C and a liquid crystalline to crystalline phase transition at 14.2°C (LC↔S). Upon heating the samples undergo two solid-solid (S↔SI) phase transitions at 2.0 and 7.2°C which probably belong to order-disorder transitions of the imidazolium alkyl chains. Then the reversible crystalline solid ↔ liquid crystalline (S↔LC) and liquid crystalline ↔ isotropic liquid (LC↔L) transitions are observed at 42.0°C and 100.2°C, respectively (Fig. 1).

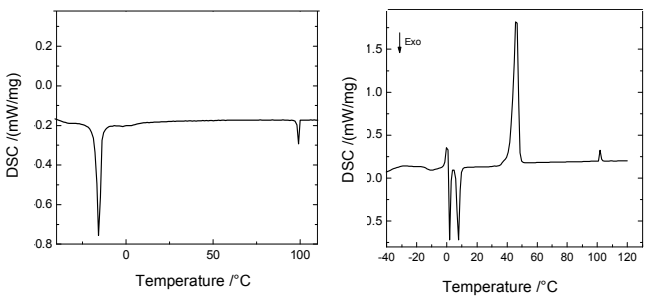

Figure 1. DSC thermograms of neat [C_{12}mim]Br. 1st cooling (left) and 2nd heating (right).

The enantiotropic liquid crystalline mesophase can be identified as a smectic A phase by polarizing optical microscopy (POM). The POM micrographs show focal conic fan textures with dark homeotropic areas. The dark homeotropic areas where no birefringens are observed when the long axis of the imidazolium cations is aligned parallel to the incident polarized light so that the light wavevector can not be rotated. The focal conic fan textures origin when a layered structure forms conical domains.

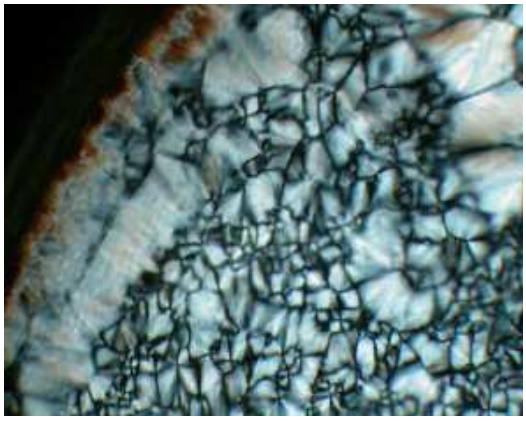

Figure 2. POM micrographs of the LC state of C_{12}mimBr.

C_{12}mimBr alone shows a bluish photoluminescence which is due to electronic transitions within the imidazolium head group. It is well known that the imidazolium π electron system can be excited with UV radiation.[36] The energy of the excited state cannot be easily converted into vibrational energy as mixing between π and σ orbitals of imidazolium is negligible and, in consequence, photoluminescence can be observed. The photoluminescence of C_{12}mimBr at λ(em) = 450 nm after excitation with λ(ex) = 366 nm is due to the allowed ($^1\pi \leftarrow {}^1\pi^*$) transition (Fig. 3). The fluorescence decay time is too short to be measured (ns regime). Phosphorescence measurements reveal a second, weaker emission which is detected at λ(em) = 515 nm for the C_{12}mim that can be assigned to the spin forbidden ($^1\pi \leftarrow {}^3\pi^*$) transition (Fig. 3). Measurements of the luminescence intensity decay reveals a lifetime of ~200 µs for the ($^1\pi \leftarrow {}^3\pi^*$) transition.

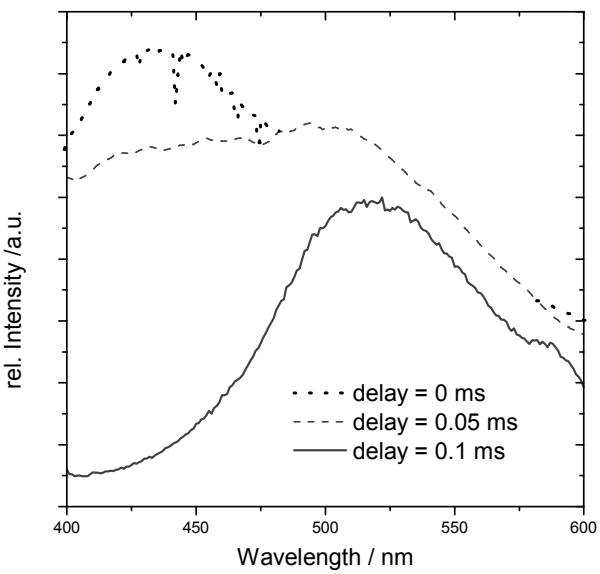

Figure 3. Photoluminescence of C_{12}mimBr at 77K, λ(ex) = 366 nm.

$EuBr_2$ in C_{12}mimBr

Figure 4 shows the thermal behaviour of C_{12}mimBr doped with different amounts of europium dibromide. All samples show the formation of a liquid crystalline state of matter. By POM measurements the mesophase can be identified as a smectic A phase (Fig. 5) similar to the mesophase formed by neat C_{12}mimBr. Samples with 0.5 and 1.0 mol% $EuBr_2$ show only small deviations with respect to their thermobehaviour when compared that of neat C_{12}mimBr. The S↔LC transitions are found at 37.6°C (0.5 mol% $EuBr_2$) and 27.5°C (1.0 mol% $EuBr_2$) compared to 38.8°C for neat C_{12}mimBr. The LC↔L transitions are detected at 98.8°C (0.5 mol% $EuBr_2$) and 101.4°C (1.0 mol% $EuBr_2$) compared to 98.6°C for neat C_{12}mimBr. Larger concentrations of $EuBr_2$ favour the LC state. In samples containing 1.9 and more mol% $EuBr_2$ the mesophasic region is extended drastically and the liquid crystalline state is even stable at room temperature and below. The LC↔L transitions occur at 0.7°C (0.9 mol% $EuBr_2$), 0.5°C (2.2 mol% $EuBr_2$) and 0.3°C (1.0 mol% $EuBr_2$). The clearing points are detected at temperatures similar to that for neat C_{12}mimBr (100 °C for 0.9 mol% $EuBr_2$, 99.5°C for 2.2 mol% $EuBr_2$ and 100.3°C for 2.9 mol% $EuBr_2$.

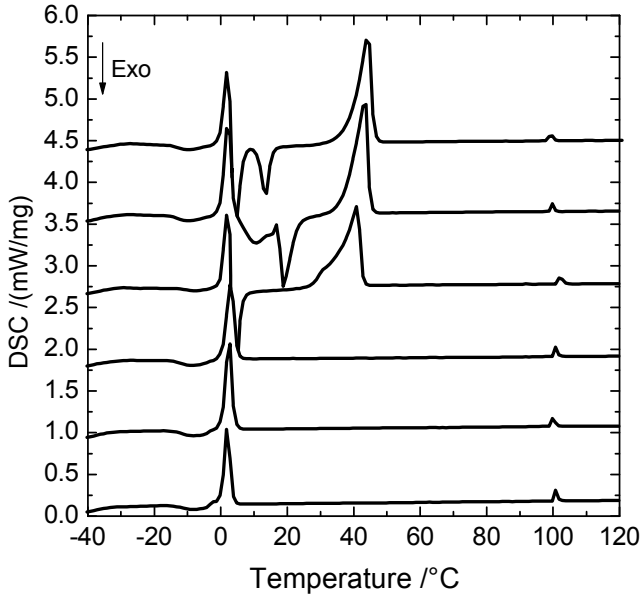

Figure 4. DSC thermograms of C_{12}mimBr (top) and C_{12}mimBr doped with different 0.5, 1.0, 1.9, 2.2 and 2.9 mol% $EuBr_2$ (from top to bottom, 2nd heating cycle).

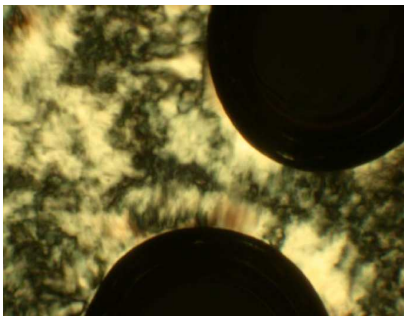

Figure 5. Typical POM micrographs of a $EuBr_2$-doped C_{12}mimBr sample in the LC state.

All $EuBr_2$ containing samples show an intense yellow color in agreement with the UV-Vis spectrum where an absorption around 420 nm can be detected (Fig. 6, left). This absorption

is due to the f→d-transition of Eu^{2+} and lies in the expected region.

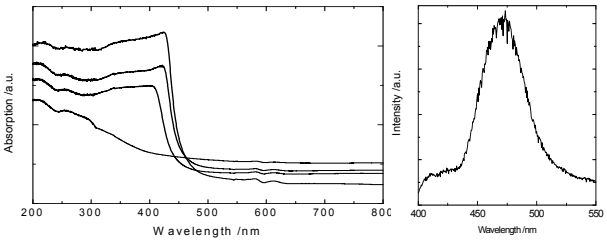

Figure 6. Left: UV-Vis absorption spectrum of C_{12}mimBr (bottom) and C_{12}mimBr doped with 0.5, 1.9 and 2.9 mol% $EuBr_2$. Right: Photoluminescence spectrum of C_{12}mimBr with 2.9 mol% $EuBr_2$ (T = 77K, λ(ex) = 350 nm).

At low temperatures (77 K) a weak blue emission of Eu^{2+} can be detected (Fig. 6, right). The emission band shows the typical quite symmetric bell shape expected for Eu^{2+}. The emission maximum upon excitation with λ(ex) = 350 nm is observed at 473 nm. This value lies between that found for $KMgBr_3$:Eu^{2+} (470 nm)[37] and $CsCdBr_3$:Eu^{2+} (476 nm)[38].

$SmBr_3$ in C_{12}mimBr

Similar to the investigations for $EuBr_2$ 1.1 mol% $SmBr_3$ was doped into C_{12}mimBr. The thermal behaviour of this sample is similar to that of C_{12}mimBr with 1.0 mol% $EuBr_2$ (Fig. 7). In this case, the smectic mesophase could be stabilized from about -9°C up to 105°C.

Low temperature photophysical investigations show aside from transitions in the π-system of imidazolium the characteristic f-f transitions of Sm^{3+} at 567 nm ($^4G_{5/2}\rightarrow{}^6H_{5/2}$), 601 nm ($^4G_{5/2}\rightarrow{}^6H_{7/2}$), 648 nm ($^4G_{5/2}\rightarrow{}^6H_{9/2}$) and 710 nm ($^4G_{5/2}\rightarrow{}^6H_{11/2}$) (Fig. 8).

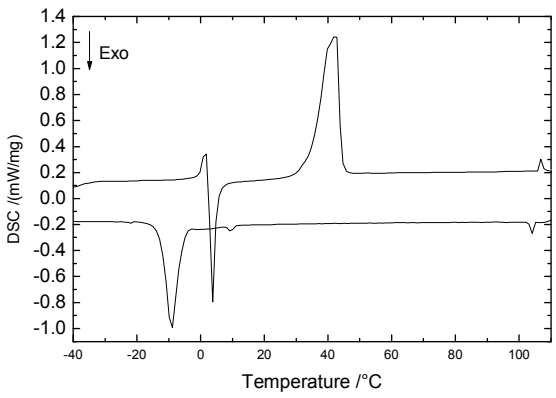

Figure 7. DSC thermogram of C_{12}mimBr with 1.1 mol% $SmBr_3$ (1st cooling (top) and 2nd heating cycle (bottom)).

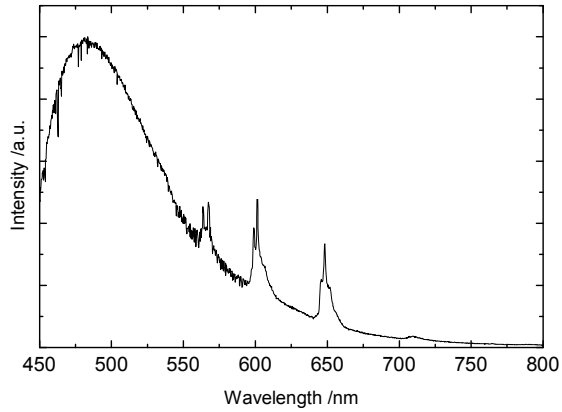

Figure 8. Emission spectrum of C_{12}mimBr with 1.1 mol% $SmBr_3$ (λ_{ex} = 310 nm, 77k).

$TbBr_3$ in C_{12}mimBr

Doping C_{12}mimBr with 1.1 mol% $TbBr_3$ yielded a liquid crystalline phase which showed a thermal behavior similar to C_{12}mimBr:Sm^{3+}. Upon cooling liquid crystalline mesophase formation is observed from about 100°C down to about -10°C (Fig. 9). Polarizing optical microscopy suggests that a smectic A phase is formed (Fig. 10).

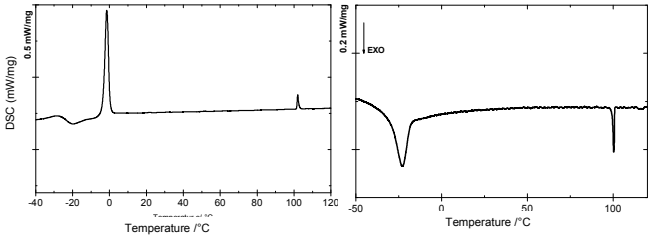

Figure 9. DSC thermogram of C_{12}mimBr with 1.0 mol% $TbBr_3$ (1st cooling (left) and 2nd heating cycle (right)).

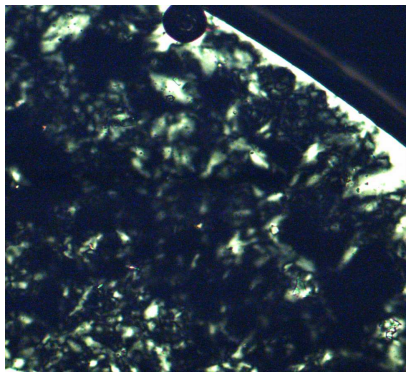

Figure 10. Typical POM micrographs of a $TbBr_3$-doped C_{12}mimBr sample in the LC state.

Strong greenish luminescence is observed (Fig. 11). The transitions occur at 488, 494 nm ($^5D_4\rightarrow{}^7F_6$), 543, 548 nm

($^4D_4 \rightarrow {}^7F_5$), 583, 590 nm ($^4D_4 \rightarrow {}^7F_4$), 620 nm ($^4D_4 \rightarrow {}^7F_3$) and 650 nm ($^4D_4 \rightarrow {}^7F_2$),.

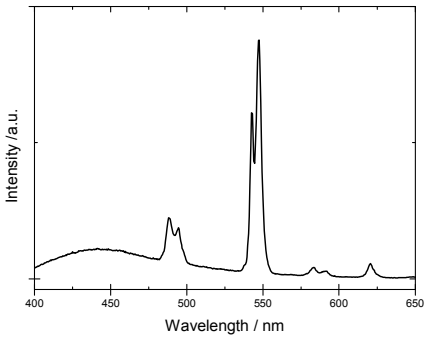

Figure 11. Emission spectrum of C_{12}mimBr with 1.1 mol% $TbBr_3$ (λ_{ex} = 310 nm, 77k).

Most interestingly the emission color of the system can be tuned by the choice of the respective excitation wavelength. While excitation with λ_{ex} = 377 nm leads to the typical yellowish-green emission of Tb^{3+}, excitation with λ_{ex} = 400 nm yields the typical white emission of C_{12}mimBr (Fig. 12, top and middle). The lifetime of the most intense f-f Tb^{3+} transition is with τ = 3.4 ms astonishingly high.

$DyBr_3$ in C_{12}mimBr

The system C_{12}mimBr:Dy^{3+} (9:1) behaves both thermally as well as photophysically similar to the analogous C_{12}mimBr:Tb^{3+} system. Again, mesophase formation is observed in the range from 100°C down to ~-10°C (Fig. 12). The textures observed by optical polarizing microscopy point to a smectic mesophase (Fig. 14).

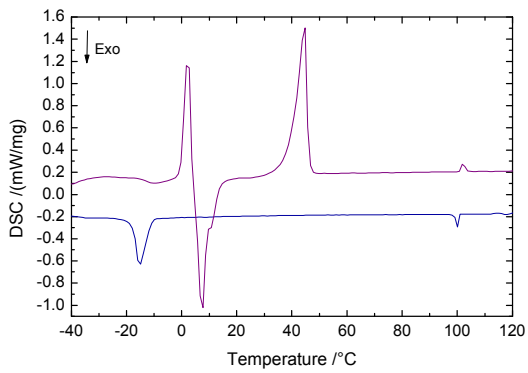

Figure 13. DSC thermogram of C_{12}mimBr: Dy^{3+}.

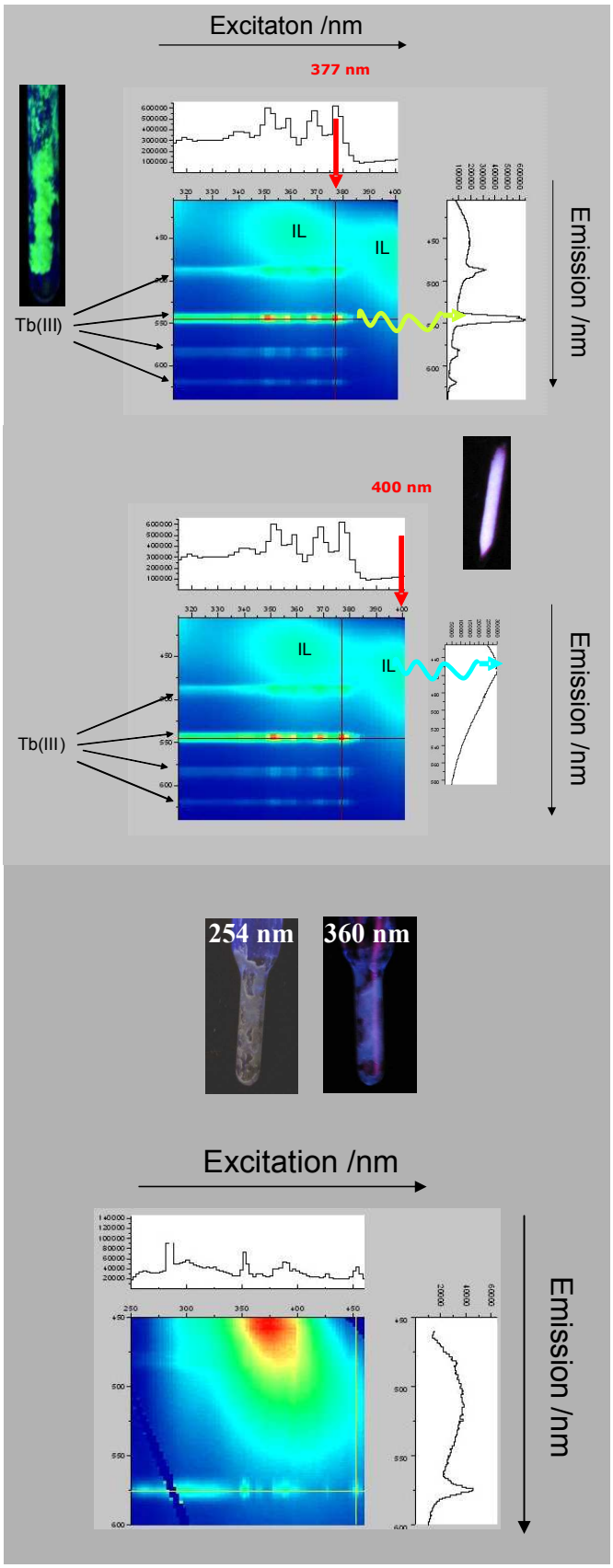

Figure 12. Top and middle: 2D excitation-emission spectra of C_{12}mimBr:Tb^{3+}; bottom: 2D excitation-emission spectra of C_{12}mimBr: Dy^{3+}. The photos show the sample under irradiation with short and longer wavelength UV light.

Figure 14. Typical POM micrographs of a $DyBr_3$-doped C_{12}mimBr sample in the LC state.

C_{12}mimBr doped with $DyBr_3$ shows strong luminescence with transitions at 578 nm ($^4F_{9/2}\rightarrow{}^6H_{13/2}$), 668 nm ($^4F_{9/2}\rightarrow{}^6H_{11/2}$) and 754 nm ($^4F_{9/2}\rightarrow{}^6F_{11/2}$, $^6H_{9/2}$) (Fig. 15).

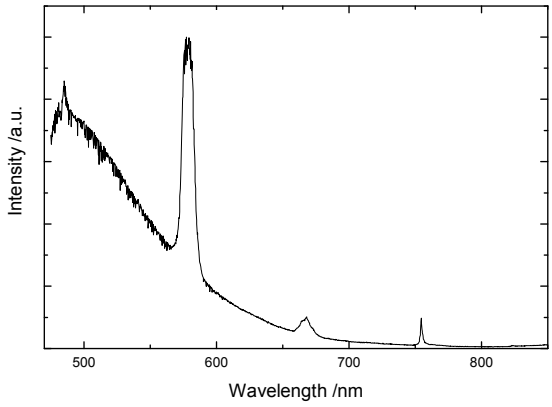

Figure 15. Emission spectrum of C_{12}mimBr with 1.1 mol% $DyBr_3$ (λ_{ex} = 310 nm, 77k).

As for $TbBr_3$ in C_{12}mimBr the emission color can be tuned by the choice of the respective excitation wavelength. While excitation with the short wavelength λ_{ex} = 254 nm leads to the characteristic yellowish emission of Dy^{3+}, excitation with λ_{ex} = 360 nm results in a bluish white emission which originates from the superposition of Dy^{3+} and C_{12}mimBr emissions (Fig. 12, bottom). The lifetime of the most intense f-f Dy^{3+} transition is determined to τ=53 µs.

Conclusions

Ln^{2+} and Ln^{3+} doped C_{12}mimBr turn out to be promising new soft optical materials. The host material C_{12}mimBr itself is an ionic liquid crystal. Lanthanide bromide dopant concentrations of up to ~1 mol% seem to have only little effect on the liquid crystalline properties of the host material. All doped materials form layered liquid crystalline mesophases even at room temperature. At the same time all compounds show reasonably good luminescence. Whilst neat C_{12}mimBr shows a bluish white emission, by doping C_{12}mimBr with $EuBr_2$ blue luminescence can be achieved. Analogous Eu^{3+} or Sm^{3+} materials show a strong red luminescence.

Of special interest is the observation, that the emission color of C_{12}mimBr doped with $TbBr_3$ and $DyBr_3$ allows for the tuning of the emission color by a mere change of the excitation light wavelength. In case of $TbBr_3$ the color can be changed between green (mainly Tb^{3+}) emission and white whereas in case of $DyBr_3$ a switch between organge-yellow and bluish white is possible. It turns out that doping C_{12}mimBr with various lanthanide bromides yields interesting new materials which show strong luminescence in the basic colors (Fig. 16) and might be used in active displays in the future.

Figure 16. Neat C_{12}mimBr (left) doped with various lanthanide bromides under UV-light.

Acknowledgements. This work was supported by the State of Nordrhein-Westfalen, the Universität zu Köln, the Ruhr-Universität Bochum as well as by the Deutsche Forschungsgemeinschaft, Bonn.

References

[1] A. Mele, G. Romano, M. Giannone, E. Ragg, G. Fronza, G. Raos, V. Marcon, *Angew. Chem. Int. Ed.* **2006**, *45*, 1123.
[2] P.J. Collings, M. Hird, *Introduction to Liquid Crystals: Chemistry and Physics*, Taylor & Francis, 1997.
[3] V.G. Chigrinov, Liquid Crystal Devices, Artech House Optoelectronic Libary, 1999.
[4] C. M. Gordon, J. D. Holbrey, A. R. Kennedy, K. R. Seddon, *J. Mater. Chem.* **1998**, *8*, 2627.
[5] E. Alami, H. Levy, R. Zana, P. Weber, A. Skoulios, *Liq. Cryst.* **1993**, *13*, 201.
[6] X. Wang, F.W. Heinemann, M. Yang, B. Melcher, M. Fekete, A.-V. Mudring, P. Wasserscheid, K. Meyer, *Chem. Commun.* **2009**, DOI: 10.1039/b914939b.
[7] S. Ujiie, K. Iimura, *Macromolecules*, **1992**, *25*, 3174.
[8] For an overview see: K. Binnemans *Chem. Rev.* **2005**, *105*, 4148.
[9] J.L. Serrano, (Ed.), *Metallomesogens, Synthesis, Properties and Applications*, Wiley-VCH, Weinheim, 1996; F. Neve, F. *Adv. Mater.* **1996**, *8*, 277; B. Donnio, D.W. Bruce, *´Metallomesogens´* in *Liquid Crystals II*, edit. by D.M.P.

Mingos, Springer, Berlin, **1999**, 193; R. Giménez, D.P. Lydon, J.L. Serrano, *Current Opinion in Solid State and Materials Science*, 2002, **6**, 527; I.J.B. Lin, C.S. Vasam, *J. Organomet. Chem.* 2005, **690**, 3498.
[10] F. Neve, *Adv. Mat.* **1996,** *8*, 277; I. J. B. Lin, C.S. Vasam, C. S. *J. Organomet. Chem.* 2005, **690**, 3498; N. Hoshino, *Coord. Chem. Rev.* **1998**, *174*, 77; P.J. Alonso, *Metallomesogens* **1996**, 387; P.J. Alonso, *Metallomesogens* **1996**, 349; P. Espinet, M.A. Esteruelas, L. A. Oro, J.L. Serrano, E. Sola, *Coord. Chem. Rev.* 1992, **117**, 215.
[11] K. Binnemans, C. Görller-Walrand, C. *Chem. Rev*. **2002**, *102*, 2303; C. Piguet, J.C.G. Bünzli, B. Donnio, D. Guillon, D. *Chem. Commun.* **2006**, 3755; E. Terazzi, S. Suarez, S. Torelli, H. Nozary, D. Imbert, O. Mamula, J.-P. Rivera, E. Guillet, J.M. Bénech, G. Bernardinelli, R. Scopelliti, B. Donnio, D. Guillon, J.-C.G. Bünzli, C. Piguet, C. *Adv. Funct. Mater*. **2006**, *16*, 157.
[12] V. Salerno, A. Grieco, M.Vacatello, *J. Phys. Chem.* **1976**, *80*, 2444.
[13] G.F. Needham, R.D. Willett, H.F. Franzen, H. F. *J. Chem. Phys.* **1984**, *88*, 674.
[14] E. Landi, M. Vacatello, M. *Thermochimica Acta* **1975**, *13*, 441.
[15] A. Kanazawa, T. Ikeda, Y. Nagase, Y. *Chem. Mater.* **2000**, *12*, 3776.
[16] K. Goossens, K.Lava, P. Nockemann, K. Van Hecke, L. Van Meervelt, P. Pattison, K. Binnemans, Th. Cardinaels, *Langmuir* **2009**, *25*, 5881; A. Getsis, A.-V. Mudring, *Z. Anorg. Allg. Chem.* **2009**, *635*, 2214.
[17] C.J. Bowlas, D.W. Bruce, K.R. Seddon, *Chem. Commun.* **1996**, 1625.
[18] F. Neve, A. Crispini, S. Armentano, O. Francescangeli, *Chem. Mater.* **1998**, *10*, 1904.
[19] F. Neve, O. Francescangeli, A. Crispini, J. Charmant, J. *Chem. Mater.* **2001**, *13*, 2032.
[20] F. Neve, O. Francescangeli, A. Crispini, A. *Inorg. Chim. Acta* **2002**, *338*, 51.
[21] F. Neve, M. Impéror-Clerc, *Liq. Cryst.* **2004**, *31*, 907.
[22] A. Taubert, *Angew. Chem. Int. Ed.* **2004**, *43*, 5380.
[23] C.K. Lee, H.H. Peng, I.J.B. Lin, I. J. B. *Chem. Mater.* **2004**, *16*, 530.
[24] A. Getsis, *Dissertation*, Universität zu Köln, 2009.
[25] A. Getsis, B. Balke, C. Felser, A.-V. Mudring, *Cryst. Growth & Des.* **2009**, *9*, 4427.
[26] A. Getsis, S. Tang, A.-V. Mudring, *Eur. J. Inorg. Chem.* 2010, in press.
[27] M.Grell, D.C. Bradley, *Adv. Mat.* 1999, **11**, 895; M. O´Neill,; S.M. Kelley, *Adv. Mat.* 2003, **15**, 1135.
[28] L.N. Puntus, K.J. Schenk, J.C.G. Bünzli, *Eur. J. Inorg. Chem.* 2005, **23**, 4739; J. Kocher, F. Gumy, A.-S. Chauvin, J.C.G. Bünzli, *J. Mat. Chem.* **2007**, *17*, 654.
[29] Y. G. Galyametdinov, A.A. Knyazev, V.I.Dzhabarov,; T. Cardinaels, K. Driesen, C. Görller-Walrand, K. Binnemans, K. *Adv.Mat.* **2008**, *20*, 252; Y.G. Galyametdinov, W. Haase, B. Goderis, D. Moors, K. Driesen, R. Van Deun, K. Binnemans, *J. Phys. Chem. B* **2007**, *111*, 13881.
[30] Y. Galyametdinov, M.A.Athanassopoulou, K. Griesar, O. Kharitonova, E.A. Soto Busmante, L. Tinchurina, I. Ovchinnikov, I.; Haase, W. *Chem. Mat.* **1996**, *8*, 922; K. Binnemans, Y.G. Galyametdinov, R. Van Deun, D.W. Bruce, S.R. Collinson, A.P. Polishchuk, I Bikchantaev, W. Haase, A.V. Prosvirin, L. Tinchurina, I Litvinov, A. Gubajdullin, A. Rakhmatullin, K. Uytterhoeven, L. Van Meervelt, *J. Am. Chem. Soc.* **2000**, *122*, 4335; V.S. Mironov, Y.G. Galyametdinov, A. Ceulemans, K. Binnemans, K. *J. Chem. Phys.* **2000**, *113*, 10293; Y.G. Galyametdinov, W. Haase, L. Malykhina, A. Prosvirin, I. Bikchantaev, A. Rakhmatullin, K. Binnemans, *Chem. Eur. J.* **2001**, *7*, 99; Y. Galyametdinov, G. Ivanova, I. Ovchinnikov, A. Prosvirin, D. Guillon, B. Heinrich, D.A. Dunmur, D.W. Bruce, *Liq. Cryst.* **1996**, *20*, 831; K. Binnemans, L. Malykhina, V.S. Mironov, W. Haase, K. Driesen, R. Van Deun, L. Fluyt, C. Görller-Walrand, Y.G. Galyametdinov, Y.G. *ChemPhysChem.* **2001**,p *2*, 680.
[31] C. Piguet, J.C.G. Bünzli, B. Donnio, D. Guillon, D. *Chem. Commun.* **2006**, 3755.
[32] A. Getsis, A.-V. Mudring, *Cryst. Res. Technol.* **2008**, *43*, 1187.
[33] G. Meyer, S. Dötsch, T. Staffel, *J. Less – Common Met*. **1987**, *127*, 155.
[34] G. Meyer, S. Dötsch, T. Staffel, *J. Less – Common Met*. **1987**, *127*, 155.
[35] G.H. Dieke, *Spectra and energy levels of rare earth ions in crystals*, Interscience Publishers, New York, **1968**; W.T. Carnall, H.M. Crosswhite, H. Crosswhite, *Energy level structure and transition probabilities in the spectra of trivalent lanthanides in* LaF_3. Special Report **1977** (Argonne, IL: Chemistry Division, Argonne National Laboratory).
[36] M.D. Lumb, *Luminescence spectroscopy*, Academic Press, London (1978).
[37] P. P. Larsen, *Dissertation*, Universität zu Köln, **2004**.
[38] F. Pelle, N. Gardant, M. Genotelle, Ph. Goldner, P. Pocher, *J. Phys. Chem. Solids* **1995**, *56*, 1003.